

Certifying Robustness of Convolutional Neural Networks with Tight Linear Approximation

Yuan Xiao
Nanjing University
Jiangsu, China
DZ21320004@smail.nju.edu.cn

Tongtong Bai
Southwest University of Science and
Technology
Sichuan, China
btt@mails.swust.edu.cn

Mingzheng Gu
Nanjing University
Jiangsu, China
MF21320043@smail.nju.edu.cn

Chunrong Fang
Nanjing University
Jiangsu, China
fangchunrong@nju.edu.cn

Zhenyu Chen
Nanjing University
Jiangsu, China
zychen@nju.edu.cn

ABSTRACT

The robustness of neural network classifiers is becoming important in the safety-critical domain and can be quantified by robustness verification. However, at present, efficient and scalable verification techniques are always sound but incomplete. Therefore, the improvement of certified robustness bounds is the key criterion to evaluate the superiority of robustness verification approaches. In this paper, we present a **Tight Linear** approximation approach for robustness verification of Convolutional Neural Networks (**Ti-Lin**). For general CNNs, we first provide a new linear constraints for S-shaped activation functions, which is better than both existing *Neuron-wise Tightest* and *Network-wise Tightest* tools. We then propose *Neuron-wise Tightest linear bounds* for Maxpool function. We implement Ti-Lin, the resulting verification method. We evaluate it with 48 different CNNs trained on MNIST, CIFAR-10, and Tiny ImageNet datasets. Experimental results show that Ti-Lin significantly outperforms other five state-of-the-art methods (CNN-Cert [2], DeepPoly [4], DeepCert [1], VeriNet [15], Newise [22]). Concretely, Ti-Lin certifies much more precise robustness bounds on pure CNNs with Sigmoid/Tanh/Arctan functions and CNNs with Maxpooling function with at most 63.70% and 253.54% improvement, respectively.

1 INTRODUCTION

Although neural networks achieve remarkable success in many complex classification tasks, such as speech and image recognition, researchers discover that non-robust neural networks are vulnerable to the perturbation from environment and adversarial attacks [10, 11, 20, 21]. In some safety-critical and security-sensitive domain, such as self-driving [12] and face recognition [13], some subtle adversarial perturbation is extremely imperceptible and harmful, and may cause disastrous consequences. Therefore, there is a great need to certify model robustness guarantees against adversarial attacks, which can provide certified defense against any possible attack [2, 6–8].

The methodology of neural network robustness verification could be divided into two categories: *complete verifier* and *incomplete verifier* [26]. *Complete verifier* [28–31] which can get accurate robustness bounds, is time-consuming and only applies to ReLU-based networks. In contrast, *incomplete verifier* [32–34] risks verification precision loss due to over-approximation but is more

scalable and efficient. Thus, to evaluate the robustness of other types of CNNs, acceleration techniques, such as linear approximation [1, 5, 9] or abstract interpretation [8, 14] is necessary. As approximation technique inevitably introduces overestimation, certified lower bound is the key criterion to evaluate robustness verification methods’ performances.

Regarding the tightness of the linear approximation technique, there is a plenty of works focusing on narrowing the input-output zone of non-linear functions in the network to gain larger certified robustness bounds [1–5, 9]. Some works propose tight linear bounds of non-linear functions by producing the minimal over-approximation zone, resulting in much more precise certified robustness bounds. Zhang et al. [22] define the linear bounds producing the minimal over-approximation area as *Neuron-wise Tightest* linear bounds. Concretely, POPQORN [3], CNN-Cert [2], and VeriNet [15] propose *Neuron-wise Tightest* robustness bounds of $\sigma(x)\tanh(y)$, $x \cdot \sigma(y)$ functions, ReLU function, and Sigmoid/Tanh/Arctan function, respectively. Recently, Zhang et al. [22] introduce the notion of *Network-wise Tightest* and propose *Network-wise Tightest* linear bounds for monotonous CNNs with Sigmoid/Tanh/Arctan function. Unfortunately, regarding the approximation methods’ performances on CNNs with Sigmoid/Tanh/Arctan function, *Neuron-wise Tightest* technique (VeriNet) is limited in precision while *Network-wise Tightest* technique (Newise [22]) is limited in scalability. Moreover, Maxpooling function is far more complex to verified as it is a multivariate function. Some attempts have been made to verify Maxpooling function but result in loose certified robustness bounds [2, 4].

To address the above challenges, in this work, we propose a **Tight Linear** approximation method called **Ti-Lin** for general CNNs. By introducing the notion of *Neuron-wise Tightest*, we discover that *Neuron-wise Tightest* is equivalent to *Layer-wise Tightest*, which can explain the reason why minimizing the area/volume between upper and lower constraints of non-linear functions can get a tighter robustness bound. We then analyze the limitations of the *Neuron-wise Tightest* and *Network-wise Tightest* techniques (VeriNet, Newise). To overcome these limitations, we make our first contribution by proposing the Tightest linear bounds for Sigmoid/Tanh/Arctan function among three state-of-the-art baseline methods. Regarding our second contribution, as mentioned above, Maxpooling is a complex function to verified. To the best of our knowledge, we

are the first to propose *Neuron-wise Tightest* linear constraints for Maxpooling function.

We implement Ti-Lin atop the state-of-the-art robustness verification framework CNN-Cert [2]. We evaluate it with neural networks trained on MNIST, CIFAR-10, and Tiny ImageNet datasets. For CNNs with Sigmoid/Tanh/Arctan functions, experimental results reveal that VeriNet [15] is superior to DeepCert [1] in 78.33% cases and Ti-Lin outperforms these two state-of-the-art techniques in 96.67% cases. Furthermore, Ti-Lin outperforms Newise, which is *Network-wise Tightest* approach with up to 63.70% improvement to certified robustness bounds. For CNNs with Maxpooling function, Ti-Lin outperforms CNN-Cert [2] and DeepPoly [4] with up to 235.54%, 43.14% improvement to certified robustness bounds, respectively. Finally, we conduct Wilcoxon rank-sum test [24] and the results confirm that Ti-Lin significantly outperform the five state-of-the-art baseline methods in precision with the same time consumption.

Compared to other related works, Ti-Lin has four significant advantages: (i) effective, it provides much tighter robustness bounds than state-of-the-art approaches, (ii) efficient, it has almost the same time consumption as other state-of-the-art techniques, (iii) versatile, it applies to general CNNs, (iv) detailed analysis and proof, it provides proofs to all theorems mentioned in this work.

In summary, our work makes the following contributions:

- We propose a **Tight Linear** approximation technique (**Ti-Lin**), which applies to general CNNs with ReLU, Sigmoid, Tanh, Arctan, and Maxpooling functions.
- We identify the limitations of existing *Neuron-wise Tightest* and *Network-wise Tightest* methods. We then propose novel linear constraints for Sigmoid/Tanh/Arctan function, which stands for the Tightest among the existing *Neuron-wise Tightest* and *Network-wise Tightest* tools.
- We first propose provably *Neuron-wise Tightest* linear constraints for Maxpool function, which significantly outperforms prior works in precision.
- We evaluate our methods on 35 different CNNs with Sigmoid/Tanh/Arctan functions and 13 types of CNNs with Maxpooling, which are both trained on MNIST, CIFAR-10 and Tiny ImageNet. The results confirm that Ti-Lin certifies more precise robustness bounds in an efficient manner than other five state-of-the-art baseline methods. We make our implementation and appendix available at <https://github.com/Ti-Lin/Ti-Lin>

The rest of this paper is organized as follows. In Section 2, we introduce some necessary preliminaries of our approach, including notations of Ti-Lin, some notions of linear approximation technique and notions of the tightness of the linear approximation technique. In Section 3, we present a technical description of Ti-Lin. We first introduce the limitation of the existing *Neuron-wise Tightest* and *Network-wise Tightest* technique which motivates us to find a tighter constraints for Sigmoid/Tanh/Arctan function. Then, we propose *Neuron-wise Tightest* linear bounds for Maxpool function and finally we present the whole computing process of our approach. In Section 4, we first introduce our experimental settings, including datasets, models and research questions and then we analyse our

Notation	Definition
$F : \mathbb{R}^{n_0} \rightarrow \mathbb{R}^{n_K}$	network classifier
n_k	number of Neurons in the k^{th} layer
$[K]$	the set $\{1, \dots, K\}$
$F_j^k(x) : \mathbb{R}^{n_0} \rightarrow \mathbb{R}$	the j^{th} output of the k^{th} layer
$L_j(x) : \mathbb{R}^{n_0} \rightarrow \mathbb{R}$	linear lower bound of $F_j^K(x)$
$U_j(x) : \mathbb{R}^{n_0} \rightarrow \mathbb{R}$	linear upper bound of $F_j^K(x)$
$L_j^k(x) : \mathbb{R}^{n_0} \rightarrow \mathbb{R}$	linear lower bound of $F_j^k(x)$
$U_j^k(x) : \mathbb{R}^{n_0} \rightarrow \mathbb{R}$	linear upper bound of $F_j^k(x)$
$a_{u,i}^k$	the slope of linear upper bound
b_u^k	the intercept of linear upper bound
$A_{U,i}^k$	the slope of $U^k(x)$
B_U^k	the intercept of $U^k(x)$
l_j^k	lower bound of $F_j^k(x)$
u_j^k	upper bound of $F_j^k(x)$
$x^k \in [l^{k-1}, u^{k-1}]$	values of neurons at the k^{th} layer
$f^k(x^{k-1}) : \mathbb{R}^{n_{k-1}} \rightarrow \mathbb{R}^{n_k}$	the function of the k^{th} layer
$Y_{L,j}$	global lower bound of $F_j^K(x)$
$Y_{U,j}$	global upper bound of $F_j^K(x)$

Table 1: Notations

experimental results. Section 5 and 6 are threats to validity and related works. Section 7 is the summary of this paper.

2 PRELIMINARIES

This section briefly introduces some related concepts and notations to understand our approach. Specially, we present the linear upper and lower bounds of convolutional and fully-connected layers, which is fundamental to our approach.

2.1 Notations

Let $F(x) : \mathbb{R}^{n_0} \rightarrow \mathbb{R}^{n_K}$ be a neural network classifier function with $(K+1)$ layers and x_0 be an input data point. We use $\sigma(\cdot)$ to denote all non-linear functions in $F(x)$. In our work, non-linear functions can be $\text{Tanh} : \sigma(x) = \frac{e^x - e^{-x}}{e^x + e^{-x}}$, $\text{Arctan} : \sigma(x) = \tan^{-1}(x)$, $\text{Sigmoid} : \sigma(x) = \frac{1}{1+e^{-x}}$, $\text{ReLU} : \sigma(x) = \max(0, x)$, $\text{Maxpool} : \sigma(x_1, \dots, x_n) = \max\{x_1, \dots, x_n\}$. We use superscripts k to denote the index of layers, subscripts u, l to denote upper and lower and subscripts $j(i, q, \text{respectively})$ denotes the $j^{th}(i^{th}, q^{th}, \text{respectively})$ Neuron of current layer. The symbols $u_j(\cdot), l_j(\cdot)$ denote the linear approximation bounding lines/planes of the j^{th} Neuron at current layer and a, b denotes the slope and intercept of linear approximation function, for example, $u_j(x) = a_{u,j}x + b_{u,j}, l_j(x) = a_{l,j}x + b_{l,j}$. We use superscripts $+, -$ to denote the positive and negative values, for example, $a^+ = \max(a, 0), a^- = \min(a, 0)$. In our approach, the global linear bounds of $F^k(x)$ are the final linear bounds to compute l^k, u^k . Other notations are in Table 1.

Let $\mathbb{B}_p(x_0, \epsilon)$ denotes x_0 perturbed within an l_p -normed ball with radius ϵ , that is $\mathbb{B}_p(x_0, \epsilon) = \{x \mid \|x - x_0\|_p \leq \epsilon\}$. t denotes the true label of x_0 in F , that is $t = \text{argmax}_i F_i(x_0)$

Definition 2.1 (Local robustness bound). if $\epsilon_r (\epsilon_r \geq 0)$ is the local robustness bound of an input x_0 in neural network, if and only if

these two conditions (i) $\operatorname{argmax}_i F_i(x) = t, \forall x \in \mathbb{B}_p(x_0, \epsilon_r)$ and (ii) $\forall \delta > 0, \exists x_a \in \mathbb{B}_p(x_0, \epsilon + \delta) s.t. \operatorname{argmax}_i F_i(x_a) \neq c$ are satisfied.

Definition 2.2 (Certified lower bound). if ϵ_{cert} is a certified lower bound of input x_0 in a neural network, if and only if these two conditions (i) $\epsilon_{cert} \leq \epsilon_r$ and (ii) $\operatorname{argmax}_i F_i(x) = t, \forall x \in \mathbb{B}_p(x_0, \epsilon_r)$.

That is to say, the local robustness bound of input x_0 is the maximum absolute safe radius of x_0 , while the certified lower bound of x_0 is the absolute safe radius of x_0 .

2.2 Linear approximation

The key idea of the linear approximation technique is to give constraints $l(x) \leq f(x) \leq u(x), x \in [l, u]$ of every layer's function $f(x)$, including non-linear, fully-connected and convolutional layers. Through propagation, the linear constraints must ensure the value of output will not exceed the upper and lower bounds, which is the key to keeping the soundness of the linear approximation technique. In our work, we fully exploit the CNNs with Maxpool and Sigmoid/Tanh/Arctan functions to give the Tightest linear constraints and make use of the general framework in CNN-Cert [2].

The procedure of computing robustness bounds is a layer-by-layer process computing from the first hidden layer to the last output layer. To compute global robustness bounds, we need to compute the linear bounds of every layer in CNNs. For details of the whole computing procedure, readers can refer to the work [4].

Definition 2.3 (Upper/Lower linear bounds). Let $f_i^k(x)$ be the function of the i^{th} Neuron in the k^{th} layer of neural network F , with $x \in [l, u] \subset \mathbb{R}^n, a_u, a_l, b_u, b_l \in \mathbb{R}^n$ and

$$u_i(x) = a_u x + b_u, l_i(x) = a_l x + b_l$$

$u_i(x)$ and $l_i(x)$ are called linear upper and lower bounds of $f_i^k(x)$ if $l_i(x) \leq f_i^k(x) \leq u_i(x), \forall x \in [l, u]$

It is worth mentioning that n is determined by the type of $f_i^k(x)$. When $f_i^k(x)$ is Maxpool function, n is equal to the size of the input to be pooled. When $f_i^k(x)$ is ReLU/Sigmoid/Tanh/Arctan function, $n = 1$. When the k^{th} layer is a convolutional layer, n corresponds to the size of the weight filter, and the linear constraints are

$$u_i(x) = w * x + b, l_i(x) = w * x + b.$$

When the k^{th} layer is a fully-connected layer, $n = n_{k-1}$ and the linear constraints are

$$u(x) = wx + b, l(x) = wx + b.$$

2.3 Tightness of linear approximation techniques

Linear approximation techniques offer an over-approximation zone of every layer's function in essence. DeepPoly [4] first discovers that minimizing the over-approximation zone can give rise to a more precise certified robustness bound. However, empirical analysis in Newise [22] shows that the linear constraints that producing the minimal over-approximation zone could not lead to the most precise robustness result all the time, which motivates us to find the relation between minimizing the over-approximation zone and Tightest robustness bound. Therefore, we introduce the notion of *Neuron-wise Tightest Linear Bounds* from Newise.

Definition 2.4 (Neuron-wise Tightest). upper linear approximation $u_i^k : \times_{q \in [n_{k-1}]} [l_q^{k-1}, u_q^{k-1}] \rightarrow \mathbb{R}$, lower linear approximation $l_i^k : \times_{q \in [n_{k-1}]} [l_q^{k-1}, u_q^{k-1}] \rightarrow \mathbb{R}$ is Neuron-wise Tightest iff $D^{k-1} = \times_{q \in [n_{k-1}]} [l_q^{k-1}, u_q^{k-1}], \forall j \in [n_{k+1}], \iint_{D^{k-1}} u_i^k(x) dx$ and $\iint_{D^{k-1}} -l_i^k(x) dx$ are minimal

We discover *Neuron-wise Tightest* linear bounds can keep the Tightest through one-layer propagation (proved in appendix). Therefore, *Neuron-wise Tightest* can explain why narrowing the over-approximation zone can increase certified robustness bounds. Furthermore, Newise defines the notion of *Network-wise Tightest*, that is, *Network-wise Tightest* linear bounds can keep the Tightest through the whole network propagation. Furthermore, Newise provides the *Network-wise Tightest* linear bounds for monotonous networks, such as non-negative networks [22].

Definition 2.5 (Network-wise Tightest). global upper linear approximation $U_i^K : \times_{q \in [n_0]} [x_{0,q} - \epsilon, x_{0,q} + \epsilon] \rightarrow \mathbb{R}$, global lower linear approximation $L_i^K : \times_{q \in [n_0]} [x_{0,q} - \epsilon, x_{0,q} + \epsilon] \rightarrow \mathbb{R}$ is network-wise Tightest iff for any different global linear constraints \hat{U}_i^K, \hat{L}_i^K ,

$$\max U_i^K(x) \leq \max \hat{U}_i^K(x), \min L_i^K(x) \geq \min \hat{L}_i^K(x), x \in \mathbb{B}_p(x_0, \epsilon)$$

3 METHODOLOGY

In this section, we present a technical description of our approach. Concretely, we first introduce our tight linear bounds for S-shaped activation function, which is tighter than both *Neuron-wise Tightest* and *Network-wise Tightest* techniques. Then, we propose *Neuron-wise Tightest* linear bounds for Maxpool function. Finally, we describe the process of computing certified robustness bounds in our approach.

3.1 Tighter Linear Bounds for S-shaped activation Functions

As approximation technique inevitably introduces imprecision, giving tighter approximation is crucial to obtaining more precise verification results. Previous works mainly provide tighter certified robustness bounds by gradually narrowing the input-output zone between the bound and linear constraint of non-linear function. Henriksen et al. [15] propose VeriNet and gives linear constraints for Sigmoid/Arctan/Tanh function by producing the minimal input-output zone. By Definition 2.4, VeriNet is the *Neuron-wise Tightest* technique for robustness verification of CNNs with Sigmoid/Arctan/Tanh function and stands for the highest precision in the sequel of narrowing the zone. As shown in Figure1, VeriNet produces smaller over-approximation zone than DeepCert, which is the most recent work.

To explain the reason why narrowing over-approximation zone can give rise to certified robustness bounds, we define *Layer-wise Tightest* linear bounds:

THEOREM 3.1 (LAYER-WISE TIGHTEST). $\forall k \in [K], i \in [n_k], m = \frac{l^{k-1} + u^{k-1}}{2}$, if both $u_i^k(m)$ and $-l_i^k(m)$ reach the minimum, then the linear upper and lower linear approximations of every non-linear function are the layer-wise Tightest.

We discover that *Layer-wise Tightest* is equivalent to *Neuron-wise Tightest* and we prove this in the Appendix. This means that

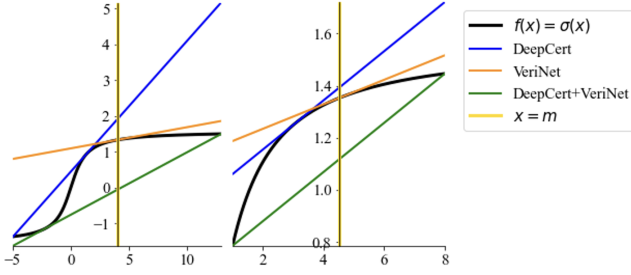


Figure 1: Linear approximation of S-shaped activation function in different $[l, u]$.

	l_p	DeepCert			VeriNet		
		l_∞	l_2	l_1	l_∞	l_2	l_1
MINST, Sig		0.03587	0.24017	0.55843	0.03594	0.24094	0.56010
CNN5_3, Tanh		0.01015	0.08234	0.20855	0.01010	0.08240	0.20970
4 layers, Atan		0.01204	0.09324	0.23936	0.01197	0.09333	0.23964
MINST, Sig		0.03482	0.20465	0.44958	0.03485	0.20515	0.45075
CNN5_3, Tanh		0.01258	0.09006	0.23889	0.01257	0.09014	0.23912
5 layers, Atan		0.00984	0.06896	0.16568	0.00983	0.06902	0.16579
MINST, Sig		0.03602	0.17939	0.35227	0.03024	0.15513	0.32903
CNN5_3, Tanh		0.00896	0.06245	0.16180	0.00822	0.05748	0.13810
6 layers, Atan		0.01202	0.07923	0.20257	0.01007	0.07339	0.18638

Table 2: Certified Robustness Bounds for l_1, l_2, l_∞ -norm perturbation by DeepCert vs. VeriNet on FNNs and CNNs, CNN5_3 denotes CNN with 5 layers and 5 filters of size 3×3

Neuron-wise Tightest can be preserved through one-layer propagation, which can explain the reason why VeriNet outperforms most previous works (such as DeepPoly [8], Neurify [35]). Zhang et al. [22] discover that VeriNet is sometimes inferior to DeepCert and we also compare these two state-of-the-art methods (results shown in Table 2). To tackle this, they define the notion of *Network-wise Tightest* and propose Newwise, the resulting method, which can preserve the tightest through the whole network propagation. However, Newwise only has the best performance on monotonous neural network (such as non-negative networks), which is not the mainstream.

To solve the above problems, we propose the Tightest linear constraints for Sigmoid/Tanh/Arctan functions among these three state-of-the-art methods (Newwise, VeriNet and DeepCert). Different from Newwise, our approach performs well on general CNNs, without limiting conditions for the weights of CNNs. Because Sigmoid, Arctan and Tanh functions satisfy when $x < 0, f''(x) > 0$; when $x > 0, f''(x) < 0$; when $x = 0, f''(x) = 0$ and are twice differentiable and centrosymmetry. Therefore, these functions are with a characteristic S shape. Due to this characteristic, these three activation functions' linear constraints are versatile in essence. We propose our linear bounds for Sigmoid/Tanh/Arctan functions:

THEOREM 3.2 (SIGMOID/TANH/ARCTAN LINEAR BOUNDS). *Supposing the k^{th} layer's function $f(x)$ is the S-shaped activation function, we define $m = F^{k-1}(x_0)$. Given $f(x), x \in [l, u]$, the linear bounds are:*

case 1: If $m \geq 0$,

$$l(x) = \begin{cases} k(x-u) + f(u), & k < f'(l) \\ f'(x^{**})(x-u) + f(u), & k \geq f'(l) \end{cases}$$

$$u(x) = \begin{cases} f'(m)(x-m) + f(m), & k_{ml} > f'(m) \\ f'(x^*)(x-l) + f(l), & k_{ml} \leq f'(m) \text{ and } k > f'(u) \\ k(x-l) + f(l), & k_{ml} \leq f'(m) \text{ and } k \leq f'(u) \end{cases}$$

case 2: If $m < 0$

$$l(x) = \begin{cases} f'(m)(x-m) + f(m), & k_{mu} \geq f'(m) \\ f'(x^{**})(x-u) + f(u), & k_{mu} < f'(m) \text{ and } k > f'(l) \\ k(x-l) + f(l), & k_{mu} < f'(m) \text{ and } k \leq f'(l) \end{cases}$$

$$u(x) = \begin{cases} k(x-u) + f(u), & k \leq f'(u) \\ f'(x^*)(x-l) + f(l), & k > f'(u) \end{cases}$$

where $k = \frac{f(u)-f(l)}{u-l}, k_{ml} = \frac{f(m)-f(l)}{m-l}, k_{mu} = \frac{f(m)-f(u)}{m-u}, x^*, x^{**}$ are tangent points, which are the solutions of these two equations: $f'(x^*) = \frac{f(x^*)-f(l)}{x^*-l}, f'(x^{**}) = \frac{f(x^{**})-f(u)}{x^{**}-u}$.

Due to the space limitation, the proof of Theorem 3.2 is deferred to Appendix. Based on Theorem 3.2, we can both efficiently and effectively obtain tight upper and lower linear bounds for Sigmoid/Tanh/Arctan function.

3.2 Neuron-wise Tightest Linear Bounds for Maxpool Function

Because Maxpool function is a multivariate function, it is far more complex to be verified compared to Sigmoid/Tanh/Arctan function. DeepPoly [4] gives non-trivial linear bounds to Maxpooling function and its parallel work, CNN-Cert [2] leverages a hyperplane containing n different particular points to give the upper and lower bound. Both these two state-of-the-art techniques fail to capture the characteristic of Maxpooling function and fail to give its *Neuron-wise Tightest* Linear Bounds, resulting in loose robustness bounds. To address this problem, we first leverage the notion of *Neuron-wise Tightest* and discover the *Neuron-wise Tightest* Linear Bounds:

THEOREM 3.3 (NEURON-WISE TIGHTEST LINEAR BOUNDS). $\forall k \in [K], i \in [n_k], m = \frac{l^{k-1}+u^{k-1}}{2}$, if both $u_i^k(m)$ and $-l_i^k(m)$ reach the minimum, then the linear upper and lower linear approximations of every non-linear function are the *Neuron-wise Tightest*.

Due to the space limitation, the proof of Theorem 3.3 is deferred to Appendix. By Theorem 3.3, we further propose Theorem 3.4 to help us find *Neuron-wise Tightest Linear Bounds* of Maxpooling function.

THEOREM 3.4 (FINDING NEURON-WISE TIGHTEST LINEAR BOUNDS). *Given that $f(x)$ is a continuous function, then*

(1) if $f'(m)(x-m) + f(m)$ is an upper(lower) bound, then $u(m)(-l(m))$ reaches its minimum.

(2) considering two points $(d_1, f(d_1)), (d_2, f(d_2))$ where $d_1, d_2 \in \times_{i=1}^n [l_i, u_i]$. When $m = \lambda d_1 + (1-\lambda)d_2, \lambda \in [0, 1]$, if the upper(lower) bounding line/plane passes through $(d_1, f(d_1)), (d_2, f(d_2))$, then $u(m)(-l(m))$ reaches its minimum.

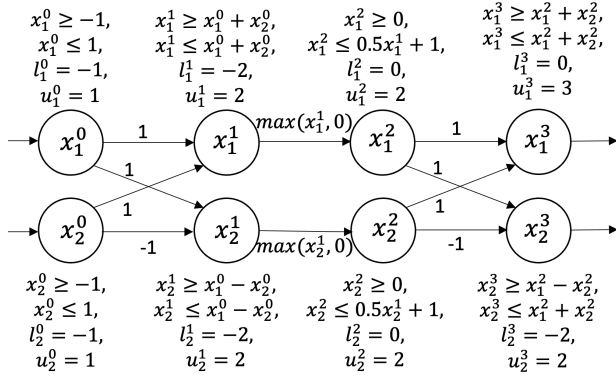


Figure 2: A toy example of how Ti-Lin computing global bounds of a FNN with one hidden-layer. For simplicity, activation function is ReLU.

Because Maxpooling function has a characteristic of piece-wise linearity, we find two particular input points of Maxpooling function which satisfy Theorem 3.4(2). These two points help us to find *Neuron-wise Tightest* upper bound. We then leverage Theorem 3.4(1) and find *Neuron-wise Tightest* lower bound. The *Neuron-wise Tightest* upper and lower bounds are presented as follows:

THEOREM 3.5 (MAXPOOL LINEAR BOUNDS). Given $f(x_1, \dots, x_n) = \max\{x_1, \dots, x_n\}$, $x_i \in [l_i, u_i]$, we first sort the elements of $\{l_i, u_i\}$, $i = 1, \dots, n$ from largest to smallest and gain the sequence q . Then the linear bounds are:

upper bound: $u(x_1, \dots, x_n) = \sum_i a_i(x_i - l_i) + b$. Specifically, there are three different cases:

case1: If $q : u_i \geq l_i \geq \dots, \forall i$, then $a_i = 1; b = l_i; a_j = 0, j \neq i$.

case2: If $q : u_i \geq u_j \geq l_j \geq \dots, \forall i, j$ or $q : u_j \geq u_i \geq l_j \geq \dots, \forall i, j$, then $a_i = \frac{u_i - l_j}{u_i - l_i}; a_j = 1; b = l_j; a_j = 0, j \neq i, j$.

case3: If $q : u_i \geq u_j \geq u_k \geq \dots, \forall i, j, k$, then $a_i = \frac{u_i - u_k}{u_i - l_i}; a_j = \frac{u_j - u_k}{u_j - l_j}; b = u_k; a_j = 0, j \neq i, j$.

lower bound: $l(x_1, \dots, x_n) = x_j, j = \operatorname{argmax}_i(m_i)$

Due to the space limitation, the proofs of Theorem 3.3 and 3.5 are deferred to Appendix. In the Appendix, we also prove that the linear bounds in Theorem 3.5 is the *Neuron-wise Tightest* Linear Bound for Maxpooling function.

3.3 Computing Certified Robustness Bounds

It consists of two parts to compute certified robustness bounds, i.e. computing global bounds for all inputs under a perturbation threshold, and computing certified robustness bounds such that all perturbed inputs have the same output classification result as the original input point.

3.3.1 Computing global bounds $\gamma_{U,j}, \gamma_{L,j}$ of network output $F_j^K(x)$. Given a K-layer CNN or FNN F , an input data point x_0 , and a perturbation threshold ϵ with l_p norm, we first compute linear bounds of each layer $f^k(x), k = 1, 2, \dots, K$ from the first hidden layer to the last output layer. We then compute the global bounds of each layer by the inequation, which are deduced by Holder's inequality:

Algorithm 1 Computing the robustness bound

Input: model F , input x , true label t ;

Output: ϵ_{cert} ;

- 1: $\epsilon \leftarrow 0.05$.
- 2: Let $\epsilon_l \leftarrow \log(\epsilon), \epsilon_{min} \leftarrow -\infty, \epsilon_{max} \leftarrow \infty$.
- 3: **for** $i=0$ to 14 **do**
- 4: Compute γ_L, γ_U of $F(x)$ with $x \in \mathbb{B}_p(x_0, \exp(\epsilon_l))$
- 5: **if** $\gamma_t^L \geq \max_{j \neq t}(\gamma_j^U)$ **then**
- 6: $\epsilon_{min} = \epsilon_l$
- 7: $\epsilon_l = \min(\epsilon_l + 1, \frac{\epsilon_{max} + \epsilon_{min}}{2})$;
- 8: **else**
- 9: $\epsilon_{max} = \epsilon_l$
- 10: $\epsilon_l = \max(\epsilon_l - 1, \frac{\epsilon_{max} + \epsilon_{min}}{2})$;
- 11: **end if**
- 12: **end for**
- 13: $\epsilon_{cert} = \exp(\epsilon_l)$
- 14: **return** ϵ_{cert}

$$F(x) \leq \epsilon \|A_U\|_q + A_U x_0 + B_U \quad (1)$$

$$F(x) \geq -\epsilon \|A_L\|_q + A_L x_0 + B_L \quad (2)$$

where $\frac{1}{q} + \frac{1}{p} = 1$. Readers can refer to the work [1] for the detailed deduction of the inequality. Note that in this paper, $p = 1, 2, \infty$.

According to the perturbation range $x \in [x_0 - \epsilon, x_0 + \epsilon]$ of input layer, we compute the linear bounds of the first hidden layer. Then, by backsubstitution [4] from current layer to the input layer and leveraging eq(1),(2) we compute the bounds $[l^1, u^1]$ of $F^1(x)$. Next, based on $[l^1, u^1]$, we can compute linear bounds of the second hidden layer and then compute the bounds $[l^2, u^2]$ by backsubstitution. This process is repeated until the global bounds $[l^K, u^K]$ (a.k.a $[\gamma_L, \gamma_U]$) of output layer is produced. To better illustrate the workflow of computing the global bounds, we cite a toy example from DeepPoly [2] of how it works on a simple FNN with one hidden-layer, two nodes of every layer and the bias set as zero (Figure 2). In Figure 2, x_i^k represents the i^{th} Neuron at the k^{th} layer. We use u_i^k, l_i^k to denote the upper and lower bounds of x_i^k , and $u_i^k(\cdot), l_i^k(\cdot)$ to denote the upper and lower linear bounds, for example, $u_2^2(x_1^1, x_2^1) = 0.5x_2^1 + 1, l_2^2(x_1^1, x_2^1) = 0$.

3.3.2 Computing certified lower bound ϵ_{cert} . We use a binary search algorithm to find the maximal certified robustness bound against all perturbed input, as shown in Algorithm 1. Concretely, we first initialize the perturbation range $\epsilon = 0.05$. To keep $\epsilon \geq 0$, we focus on the logarithm of ϵ (line 7,10). We decide whether the perturbation range is an absolute safe radius by checking whether the lower bound of $F_t(x)$ is larger than the upper bounds of $F_j(x), \forall j, j \neq t$ (line 5). If ϵ is an absolute safe radius, we increase the perturbation range (line 7); otherwise, we decrease the perturbation range (line 10). The repeat times of the binary search procedure is 15 and the difference between ϵ_{max} and ϵ_{min} is sufficiently small enough when the algorithm terminates.

4 EXPERIMENTS

We conduct extensive experiments by comparing Ti-Lin with five state-of-the-art tools (DeepCert [1], VeriNet [15], Newwise [22], CNN-Cert [2], DeepPoly [4]). The experiments run on a server running an 8 core Intel(R) Xeon(R), Silver 4114 CPU, and 15 GB of RAM with Python 3.6.13(numpy 1.19.5 with numba 0.53.1). We use the Tensorflow 1.12.0 deep learning platform to train and test CNNs.

4.1 Experiment Setups

Experiment Framework. Since the computation time of six methods may vary due to various robustness verification platform, for a fair comparison, we conduct the whole experiments and implement these six methods atop state-of-the-art robustness verification framework CNN-Cert.

Datasets. MNIST, CIFAR-10, and Tiny ImageNet are used in experiments. The MNIST[23] is a dataset of 28×28 handwritten digital images(from 0 to 9) in 10 classes. CIFAR-10 is a dataset of 60,000 $32 \times 32 \times 3$ images in 10 classes, e.g., airplane, bird, and ship. Tiny ImageNet consists of 100000 $64 \times 64 \times 3$ images in 200 classes. The value of each pixel is normalized into $[0,1]$ and thus the perturbation is in $[0,1]$.

Models. We evaluate the performance of Ti-Lin on two classes of networks: (I) pure CNNs whose activation function is Sigmoid, Tanh, or Arctan function without Maxpooling; (II) general CNNs whose activation function is ReLU function with Maxpooling and Batch Normalization. We train all CNNs on the MNIST, CIFAR-10, and Tiny ImageNet by Adam optimizer [25](50 epochs of batch size 128). Most pure CNNs(Sigmoid/Tanh/Atan) without Maxpooling use 3×3 convolutions and have five filters, while other pure CNNs use 3×3 convolutions and have 10 or 20 filters. The convolutional networks(ReLU) with Maxpooling use 32 and 64 filters for two convolution layers each.

Metrics. We refer to the metrics in CNN-Cert [2]. Concretely, we evaluate Ti-Lin and other methods on 10 random test images. As for **effectiveness**, we use $\frac{100(\epsilon'_{cert} - \epsilon_{cert})}{\epsilon_{cert}}\%$ to quantify the percentage of improvement, where ϵ'_{cert} and ϵ_{cert} represent the robustness bounds certified by Ti-Lin and other comparative tools, respectively. We color result tables' cells in orange from light to dark by checking whether the value of improvement(%) is in $[0, 20)$, $[20, 40)$, $[40, 60)$, or $[60, +\infty)$. As for **efficiency**, we record the average computation time over the correctly-classified images.

4.2 Research Questions

To check whether Ti-Lin is the Tightest linear approximation technique for Sigmoid/Tanh/Arctan function among existing *Neuron-wise Tightest* linear approximation approach(VeriNet) and *Network-wise Tightest* approach(Newwise), we propose two research questions which are listed as follows:

- **RQ1(vs. Neuron-wise Tightest Approach)** : Whether Ti-Lin outperforms Neuron-wise Tightest technique on various networks in different datasets perturbed in l_1, l_2, l_∞ norm and overcomes the aforementioned limitation of Neuron-wise Tightest technique?

- **RQ2(vs. Network-wise Tightest Approach)**: Whether Ti-Lin outperforms Network-wise Tightest technique on various networks in different datasets perturbed in l_1, l_2, l_∞ norm?

To check whether Ti-Lin, the *Neuron-wise Tightest* method for Maxpooling function, stands for the highest precision of certifying robustness bounds among DeepPoly and CNN-Cert, we propose the following research question:

- **RQ3(vs. State-of-the-art)** :Whether Ti-Lin outperforms State-of-the-art techniques on various networks in different datasets perturbed in l_1, l_2, l_∞ norm?

Finally, we propose the following research question:

- **RQ4(Significant Improvement)**:Is the improvement of Ti-Lin statistically significant compared to all baseline methods?

4.3 RQ1(vs. Neuron-wise Tightest Approach)

We answers **RQ1** by comparing our approach with VeriNet(*Neuron-wise Tightest* technique) and DeepCert, which are the two most recent methods.

Table 3 and Table 4 show the results of certified lower bounds computed by these three methods for pure convolutional networks with three different activation functions on the MNIST and CIFAR-10 datasets, respectively. The best one' cell is colored in orange.

Compared to the results in Table 2, Table 3 shows that Ti-Lin has overcome the limitation of *Neuron-wise Tightest* Approach(VeriNet). Concretely, in Table 3 and 4 Ti-Lin outperforms both VeriNet and DeepCert in 96.67% and 93.33% cases, respectively, while VeriNet outperforms DeepCert in 78.33% cases on MNIST dataset. The only five bad results in Table 3 happen in CNNs with four layers and Sigmoid network with 6 layers. However, when the number of layers increases, the superiority of Ti-Lin plays a more and more important role in tightening certified robustness bound and thus the bounds certified by Ti-Lin become larger than other two baseline methods. Some sigmoid networks' results are omitted due to poor test set accuracy. As for time efficiency, these three methods cost almost the same time for the same network architectures.

4.4 RQ2(vs. Network-wise Tightest Approach)

We answers **RQ2** by comparing our approach with Newwise(*Network-wise Tightest* technique), which stands for the highest precision for monotonous networks.

Table 5 and 6 show the results of certified lower bounds for 36 different pure convolutional networks with three types of activation functions on the MNIST and CIFAR-10 dataset respectively. As shown in Table 5 and 6, in 94.29% cases, Ti-Lin can compute much larger robustness bounds with up to 63.70% and 43.66% improvement than Newwise. Ti-Lin is inferior to Newwise in some sigmoid networks against l_∞ -norm perturbation. The reason is that Sigmoid function's value is non-negative, which is different from Tanh and Arctan functions and this makes the weights of the network prone to be non-negative. Moreover, Newwise is the Tightest approximation technique for non-negative networks and therefore has better performance than Ti-Lin. However, the proportion of bad results is only 5.71%. Regarding time efficiency, Ti-Lin costs almost the

Network	Certified Bounds									Average Computation Time(sec)									
	l_p	DeepCert			VeriNet			Ti-Lin			DeepCert			VeriNet			Ti-Lin		
		l_∞	l_2	l_1	l_∞	l_2	l_1	l_∞	l_2	l_1	l_∞	l_2	l_1	l_∞	l_2	l_1	l_∞	l_2	l_1
MNIST	Sig	0.03587	0.24017	0.55843	0.03594	0.24094	0.5601	0.03606	0.24209	0.56207	6.85	6.69	6.7	6.78	6.7	6.74	7.63	6.77	6.62
CNN5_3	Tanh	0.01015	0.08234	0.20855	0.0101	0.0824	0.2097	0.0101	0.08243	0.20976	6.82	6.84	6.82	6.83	6.74	6.74	6.89	6.72	6.71
4 layer	Atan	0.01204	0.09324	0.23936	0.01197	0.09333	0.23964	0.01198	0.09338	0.23976	6.55	6.44	6.61	6.68	6.69	6.79	6.87	6.68	6.7
MNIST	Sig	0.03482	0.20465	0.44958	0.03485	0.20515	0.45075	0.03502	0.20672	0.45423	16.42	16.37	18.75	16.17	16.42	17.95	16.83	16.02	17.45
CNN5_3	Tanh	0.01258	0.09006	0.23889	0.01257	0.09014	0.23912	0.01259	0.09034	0.23967	16.49	17.5	18.29	16.06	16.41	18.17	16.28	16.14	18.15
5 layer	Atan	0.00984	0.06896	0.16568	0.00983	0.06902	0.16579	0.00985	0.06913	0.16598	16	18.13	18.17	15.95	17.85	18.12	16.21	16.36	17.79
MNIST	Sig	0.03602	0.17939	0.35227	0.03024	0.15513	0.32903	0.03645	0.18177	0.35641	31.98	32.89	31.96	32.30	33.33	32.72	32.8	34.17	32.27
CNN5_3	Tanh	0.00896	0.06245	0.1618	0.00822	0.05748	0.1381	0.00901	0.06278	0.16269	32.35	32.24	32.21	32.25	32.48	32.87	32.53	32.22	33.14
6 layer	Atan	0.01202	0.07923	0.20257	0.01007	0.07339	0.18638	0.01207	0.07956	0.2032	32.44	33.45	33.39	32.57	32.42	32.65	32.53	32.32	32.12
MNIST	Sig	0.06192	0.23208	0.41802	0.06263	0.23518	0.42313	0.06317	0.23764	0.42798	55.81	55.67	53.77	59.19	55.75	62.80	54.4	56.03	54.5
CNN5_3	Tanh	0.00899	0.06489	0.17935	0.00904	0.06508	0.17953	0.00907	0.06531	0.18016	54.23	54.39	55.69	55.11	55.09	55.61	54.63	54.78	54.92
7 layer	Atan	0.01124	0.07608	0.18589	0.01128	0.07637	0.1864	0.01131	0.07655	0.1869	55.2	54.96	55.08	55.34	58.65	55.61	54.51	54.45	54.69
MNIST	Sig	0.04335	0.1833	0.3564	0.04387	0.18567	0.3608	0.04433	0.18774	0.3648	84.3	82.28	81.01	83.63	82.65	83.20	85.13	88.17	82.53
CNN5_3	Tanh	0.00961	0.06128	0.14527	0.00965	0.06149	0.14567	0.0097	0.06181	0.14644	81.81	84.24	83.91	83.62	83.71	84.56	82.86	82.8	83.14
8 layer	Atan	0.01001	0.06736	0.17055	0.01004	0.06764	0.17122	0.01007	0.06784	0.17177	83.25	83.02	80.2	83.67	83.83	84.10	82.54	82.8	82.47
MNIST	Sig	0.03149	0.15305	0.31889	0.03163	0.15385	0.32056	0.03184	0.15492	0.32251	158.9	159.99	169.07	161.60	160.56	159.25	163.1	158.97	158.93
CNN10_3	Tanh	0.00739	0.04488	0.10848	0.00744	0.04524	0.10934	0.00746	0.04535	0.10964	159.68	160.31	169.27	160.18	160.01	160.15	159.08	159.6	159.12
8 layer	Atan	0.00581	0.03499	0.08051	0.00588	0.03543	0.08148	0.00589	0.0355	0.08163	159.09	165.78	166.73	160.60	160.84	160.59	158.92	163.08	158.61
MNIST	Sig	-	-	-	-	-	-	-	-	-	-	-	-	-	-	-	-	-	-
CNN20_3	Tanh	0.00507	0.02932	0.06925	0.00512	0.02966	0.07009	0.00513	0.0297	0.07018	427.14	427.65	423.69	423.27	424.76	408.56	401.54	408.79	404.25
8 layer	Atan	0.00581	0.03315	0.07906	0.00592	0.03376	0.08042	0.00593	0.03381	0.08057	419.33	420.43	414.76	413.13	414.5	408.8	404.26	409.78	409.43

Table 3: Averaged certified robustness bounds and runtime on pure CNNs tested on MNIST by DeepCert, VeriNet and Ti-Lin

Network	Certified Bounds									Average Computation Time(sec)									
	l_p	DeepCert			VeriNet			Ti-Lin			DeepCert			VeriNet			Ti-Lin		
		l_∞	l_2	l_1	l_∞	l_2	l_1	l_∞	l_2	l_1	l_∞	l_2	l_1	l_∞	l_2	l_1	l_∞	l_2	l_1
CIFAR	Sig	0.0048	0.07464	0.29181	0.00479	0.07456	0.29177	0.0048	0.07487	0.29242	27.27	27.19	27.35	29.12	28.86	29.64	27.97	27.51	27.99
CNN5_3	Tanh	0.0021	0.03887	0.13322	0.0021	0.03886	0.13323	0.0021	0.03887	0.13325	27.47	27.42	27.47	30.01	28.95	29.04	27.46	27.69	27.81
5 layer	Atan	0.00232	0.04134	0.14716	0.00232	0.04135	0.14734	0.00232	0.04135	0.14734	26.81	26.97	27.11	28.85	29.04	29.4	28.3	27.61	28.03
CIFAR	Sig	0.00778	0.10585	0.38266	0.00778	0.10589	0.3829	0.00777	0.10539	0.38016	102.03	113.12	108.31	99.03	105.53	96.09	111.07	120.69	114.31
CNN5_3	Tanh	0.00081	0.02575	0.12023	0.00081	0.02575	0.12041	0.00081	0.02575	0.12041	123.38	114.89	105.78	94.17	90.55	88.37	104.48	119.65	104.61
6 layer	Atan	0.00094	0.02812	0.12944	0.00094	0.02813	0.12964	0.00094	0.02813	0.12964	103.85	113.59	106.33	94.22	99.01	97.13	99.16	106.91	106.49
CIFAR	Sig	0.02036	0.16852	0.52567	0.02046	0.1693	0.52814	0.02081	0.17176	0.53537	151.43	160.8	133.69	125.68	124.27	129.50	145.4	147.03	145.07
CNN5_3	Tanh	0.00078	0.02222	0.10962	0.00078	0.02222	0.10982	0.00078	0.02222	0.10982	139.93	146.92	127.9	124.18	125.57	123.87	134.31	145.56	140.34
7 layer	Atan	0.00116	0.02897	0.12481	0.00116	0.02897	0.12494	0.00116	0.02898	0.12494	145.71	145.62	129.86	123.64	124.82	123.9	149.02	149.44	144.26
CIFAR	Sig	-	-	-	-	-	-	-	-	-	-	-	-	-	-	-	-	-	-
CNN5_3	Tanh	0.00156	0.02907	0.09497	0.00156	0.02908	0.09505	0.00156	0.02908	0.09506	187	179.6	171.34	172.47	174.26	171.19	185.86	181.71	177.3
8 layer	Atan	0.001	0.02564	0.11059	0.001	0.02564	0.1107	0.001	0.02564	0.1107	178.97	175.3	175.13	170.41	170.97	173.10	181.46	176.01	177.86
CIFAR	Sig	-	-	-	-	-	-	-	-	-	-	-	-	-	-	-	-	-	-
CNN5_3	Tanh	0.001	0.02078	0.08589	0.001	0.02078	0.08591	0.001	0.02078	0.08592	183.02	182.47	182.65	180.85	180.57	180.79	194.67	188.13	191.04
9 layer	Atan	0.00119	0.02175	0.08199	0.00119	0.02175	0.082	0.00119	0.02176	0.08202	181.3	181.41	181.45	180.56	181.11	181.39	191.16	190.61	188.62
CIFAR	Sig	-	-	-	-	-	-	-	-	-	-	-	-	-	-	-	-	-	-
CNN10_3	Tanh	0.00096	0.02518	0.11476	0.00096	0.02518	0.11476	0.00096	0.02519	0.1149	581.81	586.82	586.2	531	572.75	570.55	585.05	592.39	588.48
8 layer	Atan	0.00074	0.02172	0.11343	0.00074	0.02172	0.11343	0.00074	0.02173	0.11366	546.31	579.98	507.19	528.93	497.72	575.7	552.37	466.9	550.25

Table 4: Averaged certified robustness bounds and runtime on pure CNNs tested on CIFAR-10 by DeepCert, VeriNet and Ti-Lin

same time as Newise. In conclusion, Ti-Lin is the best linear approximation approach for general CNNs among DeepCert, VeriNet and Newise.

4.5 RQ3(vs. State-of-the-art)

We answer RQ3 by comparing our approach with the two promising methods(CNN-Cert, DeepPoly) as baselines.

Table 7, 8 and 9 show the results of certified lower bounds for general convolutional networks(ReLU) with Maxpooling on MNIST, CIFAR-10 dataset, and Tiny ImageNet respectively. Ti-Lin can compute much larger robustness bounds with up to 235.54%

improvement than CNN-Cert and 43.14% improvement than DeepPoly, which further confirms that *Neuron-wise Tightest* technique can give rise to tighter robustness bounds. As for time efficiency, Ti-Lin costs almost the same time as DeepPoly and CNN-Cert for the same network architecture due to their common framework CNN-Cert.

4.6 RQ4(Significant Improvement)

We answer RQ4 by applying Wilcoxon Rank-sum Test(a.k.a Mann-Whitney U test) [24] at the significance level of 0.05. We suppose Y, T are continuous random variables and represent the

Network	Certified Bounds						Ti-Lin Impr.(%)			Average Computation Time(second)						
	l_p	Newise			Ti-Lin			vs. Newise			VeriNet			Ti-Lin		
		l_∞	l_2	l_1	l_∞	l_2	l_1	l_∞	l_2	l_1	l_∞	l_2	l_1	l_∞	l_2	l_1
MNIST	Sig	0.03715	0.2165	0.48434	0.0361	0.2421	0.5621	-2.93 ↓	11.82 ↑	16.05 ↑	6.61	6.66	6.58	7.63	6.77	6.62
CNN5_3	Tanh	0.00901	0.05944	0.1417	0.0101	0.0824	0.2098	12.10 ↑	38.68 ↑	48.03 ↑	6.57	6.72	6.68	6.89	6.72	6.71
4 layer	Atan	0.01079	0.06836	0.16643	0.0120	0.0934	0.2398	11.03 ↑	36.60 ↑	44.06 ↑	6.52	6.6	6.58	6.87	6.68	6.7
MNIST	Sig	0.03593	0.18297	0.38635	0.0350	0.2067	0.4542	-2.53 ↓	12.98 ↑	17.57 ↑	15.85	16.1	15.8	16.83	16.02	17.45
CNN5_3	Tanh	0.01115	0.06868	0.173	0.0126	0.0903	0.2397	12.91 ↑	31.54 ↑	38.54 ↑	16.5	15.98	15.78	16.28	16.14	18.15
5 layer	Atan	0.0085	0.05174	0.11899	0.0099	0.0691	0.1660	15.88 ↑	33.61 ↑	39.49 ↑	15.95	15.88	15.67	16.21	16.36	17.79
MNIST	Sig	0.02898	0.13453	0.27428	0.0365	0.1818	0.3564	25.78 ↑	35.11 ↑	29.94 ↑	31.84	31.78	32.46	32.8	34.17	32.27
CNN5_3	Tanh	0.00701	0.04351	0.09938	0.0090	0.0628	0.1627	28.53 ↑	44.29 ↑	63.70 ↑	31.9	32.51	31.9	32.53	32.22	33.14
6 layer	Atan	0.00862	0.05596	0.13531	0.0121	0.0796	0.2032	40.02 ↑	42.17 ↑	50.17 ↑	31.95	31.9	32.02	32.53	32.32	32.12
MNIST	Sig	0.06872	0.22792	0.38977	0.0632	0.2376	0.4280	-8.08 ↓	4.26 ↑	9.80 ↑	53.69	54.51	54.42	54.4	56.03	54.5
CNN5_3	Tanh	0.00765	0.04997	0.13122	0.0091	0.0653	0.1802	18.56 ↑	30.70 ↑	37.30 ↑	53.83	53.94	54.13	54.63	54.78	54.92
7 layer	Atan	0.00948	0.05808	0.13547	0.0113	0.0766	0.1869	19.30 ↑	31.80 ↑	37.96 ↑	54.01	54.34	53.76	54.51	54.45	54.69
MNIST	Sig	0.04683	0.17735	0.33256	0.0443	0.1877	0.3648	-5.34 ↓	5.86 ↑	9.69 ↑	81.45	88.06	81.83	85.13	88.17	82.53
CNN5_3	Tanh	0.00797	0.04658	0.10542	0.0097	0.0618	0.1464	21.71 ↑	32.70 ↑	38.91 ↑	81.69	81.52	82.36	82.86	82.8	83.14
8 layer	Atan	0.00823	0.05105	0.12405	0.0101	0.0678	0.1718	22.36 ↑	32.89 ↑	38.47 ↑	86.48	81.7	81.72	82.54	82.8	82.47
MNIST	Sig	0.03095	0.13464	0.26974	0.0318	0.1549	0.3225	2.88 ↑	15.06 ↑	19.56 ↑	161.2	162.11	161.68	163.1	158.97	158.93
CNN10_3	Tanh	0.00584	0.03324	0.07814	0.0075	0.0454	0.1096	27.74 ↑	36.43	40.31	163.16	161.57	162.99	159.08	159.6	159.12
8 layer	Atan	0.00441	0.02512	0.0564	0.0059	0.0355	0.0816	33.56 ↑	41.32	44.73 ↑	161.03	161.69	162.98	158.92	163.08	158.61
MNIST	Sig	-	-	-	-	-	-	-	-	-	-	-	-	-	-	-
CNN20_3	Tanh	0.00372	0.02066	0.04802	0.0051	0.0297	0.0702	37.90 ↑	43.76 ↑	46.15 ↑	432.55	417.85	415.31	401.54	408.79	404.25
8 layer	Atan	0.00445	0.02424	0.05654	0.0059	0.0338	0.0806	33.26 ↑	39.48 ↑	42.50 ↑	425.37	413.34	413.98	404.26	409.78	409.43

Table 5: Averaged certified robustness bounds and runtime on pure CNNs tested on MNIST by Newise and Ti-Lin

Network	Certified Bounds						Ti-Lin Impr.(%)			Average Computation Time(second)						
	l_p	Newise			Ti-Lin			vs. Newise			VeriNet			Ti-Lin		
		l_∞	l_2	l_1	l_∞	l_2	l_1	l_∞	l_2	l_1	l_∞	l_2	l_1	l_∞	l_2	l_1
CIFAR	Sig	0.00473	0.06054	0.21678	0.0048	0.07487	0.29242	1.48 ↑	23.67 ↑	34.89 ↑	29.12	28.86	29.64	27.97	27.51	27.99
CNN5_3	Tanh	0.00197	0.02957	0.09394	0.0021	0.03887	0.13325	6.60 ↑	31.45 ↑	41.85 ↑	30.01	28.95	29.04	27.46	27.69	27.81
5 layer	Atan	0.00216	0.03078	0.10256	0.00232	0.04135	0.14734	7.41 ↑	34.34 ↑	43.66 ↑	28.85	29.04	29.40	28.30	27.61	28.03
CIFAR	Sig	0.00793	0.08821	0.29653	0.00777	0.10539	0.38016	-2.02 ↓	19.48 ↑	28.20 ↑	104.25	121.23	104.56	111.07	120.69	114.31
CNN5_3	Tanh	0.0008	0.0222	0.08789	0.00081	0.02575	0.12041	1.25 ↑	15.99 ↑	37.00 ↑	120.08	105.66	106.15	104.48	119.65	104.61
6 layer	Atan	0.00093	0.0237	0.09422	0.00094	0.02813	0.12964	1.08 ↑	18.69 ↑	37.59 ↑	119.15	118.06	114.62	99.16	106.91	106.49
CIFAR	Sig	0.02172	0.16076	0.47508	0.02081	0.17176	0.53537	-4.19 ↓	6.84 ↑	12.69 ↑	145.41	149.28	136.21	145.4	147.03	145.07
CNN5_3	Tanh	0.00077	0.0185	0.07987	0.00078	0.02222	0.10982	1.30 ↑	20.11 ↑	37.50 ↑	149.42	136.88	134.65	134.31	145.56	140.34
7 layer	Atan	0.00113	0.02334	0.09015	0.00116	0.02898	0.12494	2.65 ↑	24.16 ↑	38.59 ↑	149.67	126.95	139.84	149.02	149.44	144.26
CIFAR	Sig	-	-	-	-	-	-	-	-	-	216.77	204.66	193.63	97.62	91.6	88.71
CNN5_3	Tanh	0.00147	0.02218	0.06738	0.00156	0.02908	0.09506	6.12 ↑	31.11 ↑	41.08 ↑	177.03	173.17	171.51	185.86	181.71	177.3
8 layer	Atan	0.00098	0.02146	0.0814	0.001	0.02564	0.1107	2.04 ↑	19.48 ↑	36.00 ↑	173.27	174.95	171.16	181.46	176.01	177.86
CIFAR	Sig	-	-	-	-	-	-	-	-	-	-	-	-	-	-	-
CNN5_3	Tanh	0.00093	0.01631	0.06166	0.001	0.02078	0.08592	7.53 ↑	27.41 ↑	39.34 ↑	179.14	182.18	180.04	194.67	188.13	191.04
9 layer	Atan	0.0011	0.01663	0.05847	0.00119	0.02176	0.08202	8.18 ↑	30.85 ↑	40.28 ↑	179.71	180.24	179.85	191.16	190.61	188.62
CIFAR	Sig	-	-	-	-	-	-	-	-	-	-	-	-	-	-	-
CNN10_3	Tanh	0.00094	0.02083	0.08419	0.00096	0.02519	0.1149	2.13 ↑	20.93 ↑	36.48 ↑	578.9	558.31	563.76	585.05	592.39	588.48
8 layer	Atan	0.00073	0.01897	0.08388	0.00074	0.02173	0.11366	1.37 ↑	14.55 ↑	35.50 ↑	534.42	496.85	490.54	552.37	466.9	550.25

Table 6: Averaged certified robustness bounds and runtime on pure CNNs tested on CIFAR-10 by Newise and Ti-Lin

robustness bound certified by baseline method and Ti-Lin, respectively. To check whether the improvement of Ti-Lin in the above results is significant compared to the five state-of-the-art baseline methods, we consider the statistic:

$$W = \#\{(T_i, Y_i) : T_i > Y_i; i = 1, \dots, n\}$$

where n is the number of samples. Therefore, we define B as a continuous random variable representing the difference between Ti-Lin and the baseline method $T - Y$. We define Z as another random variable and $P(Z = 0) = 1$. The null hypothesis is that B and Z are equal in distribution and alternative hypothesis is that B

is stochastically strictly greater than Z :

$$H_0 : B \stackrel{d}{=} Z \text{ versus } H_1 : B >_{st} Z$$

Table 10 contains the results of Wilcoxon Rank-sum Test, which reject H_0 and confirm that Ti-Lin significantly performs better than any one of the five state-of-the-art baseline methods across different network architectures on various datasets.

5 THREATS TO VALIDITY

We discuss potential threats to the validity of this paper in terms of its application domains.

Network	l_p	Certified Bounds			Ti-Lin Impr.(%)		Average Runtime(second)		
		CNN-Cert	DeepPoly	Ti-Lin	vs. CNN-Cert	vs. DeepPoly	CNN-Cert	DeepPoly	Ti-Lin
MNIST	l_∞	0.01318	0.02277	0.02569	94.92↑	12.82↑	105.75	99.62	104.42
CNN	l_2	0.04427	0.08888	0.10647	140.50↑	19.79↑	83.45	81.06	84.84
4 layer	l_1	0.08544	0.17689	0.21507	151.72↑	21.58↑	83.03	81.73	85.58
MNIST	l_∞	0.01288	0.02057	0.02382	84.94↑	15.80↑	506.17	528.11	508.01
CNN	l_2	0.05164	0.08445	0.09867	91.07↑	16.84↑	713.8	486	825.79
5 layer	l_1	0.10147	0.16244	0.18877	86.04↑	16.21↑	646.46	486	505.46
MNIST	l_∞	0.01025	0.0163	0.01848	80.29↑	13.37↑	227.7	230.53	226.69
CNN	l_2	0.03954	0.06473	0.0729	84.37↑	12.62↑	233.77	230.62	234.5
6 layer	l_1	0.07708	0.12361	0.13894	80.25↑	12.40↑	235.9	230.76	234.91
MNIST	l_∞	0.00647	0.01241	0.01383	113.76↑	11.44↑	274.17	260.64	264.99
CNN	l_2	0.02733	0.05875	0.06572	140.47↑	11.86↑	274.86	261.3	274.53
7 layer	l_1	0.05443	0.11925	0.1331	144.53↑	11.61↑	271.96	262.35	273.25
MNIST	l_∞	0.00847	0.01312	0.01655	95.40↑	26.14↑	289.08	298.85	293.12
CNN	l_2	0.03751	0.05789	0.07124	89.92↑	23.06↑	291.67	325.52	292.86
8 layer	l_1	0.07515	0.11376	0.1383	84.03↑	21.57↑	292.05	340.22	291.42

Table 7: Averaged certified robustness bounds and runtime on CNNs(ReLU) with Maxpooling tested on MNIST by CNN-Cert, DeepPoly and Ti-Lin

Network	l_p	Certified Bounds			Ti-Lin Impr.(%)		Average Runtime(second)		
		CNN-Cert	DeepPoly	Ti-Lin	vs. CNN-Cert	vs. DeepPoly	CNN-Cert	DeepPoly	Ti-Lin
CIFAR	l_∞	0.00108	0.00162	0.0019	75.93↑	17.28↑	151.98	158.63	162.54
CNN	l_2	0.00751	0.01655	0.02332	210.52↑	40.91↑	153.19	160.23	163.34
4 layer	l_1	0.02127	0.04986	0.07137	235.54↑	43.14↑	152.16	156.71	163.34
CIFAR	l_∞	0.00115	0.00175	0.00211	83.48↑	20.57↑	817.49	775.74	796.36
CNN	l_2	0.00953	0.0176	0.0236	147.64↑	34.09↑	780.93	761.15	791.13
5 layer	l_1	0.0285	0.05459	0.0732	156.84↑	34.09↑	783.2	774.19	805.72
CIFAR	l_∞	0.00099	0.00144	0.0017	71.72↑	18.06↑	353.38	374.11	366.72
CNN	l_2	0.0083	0.01301	0.0163	96.39↑	25.29↑	356.44	363.89	355.38
6 layer	l_1	0.02387	0.03794	0.04797	100.96↑	26.44↑	356.91	369.94	352.09
CIFAR	l_∞	0.00066	0.00082	0.001	51.52↑	21.95↑	395.46	416.51	408.75
CNN	l_2	0.00573	0.00761	0.00995	73.65↑	30.75↑	401.45	418.47	410.17
7 layer	l_1	0.01673	0.02271	0.02975	77.82↑	31.00↑	393.44	417.33	395.37
CIFAR	l_∞	0.00056	0.0009	0.00106	89.29↑	17.78↑	511.38	465.3	507.67
CNN	l_2	0.00536	0.00863	0.01099	105.04↑	27.35↑	447.3	450.49	449.19
8 layer	l_1	0.01609	0.02574	0.03354	108.45↑	30.30↑	443.38	448.39	445.2

Table 8: Averaged certified robustness bounds and runtime on CNNs(ReLU) with Maxpooling tested on CIFAR-10 by CNN-Cert, DeepPoly and Ti-Lin

Network	l_p	Certified Bounds			Ti-Lin Impr.(%)		Average Runtime(second)		
		CNN-Cert	DeepPoly	Ti-Lin	vs. CNN-Cert	vs. DeepPoly	CNN-Cert	DeepPoly	Ti-Lin
Tiny ImageNet	l_∞	0.00051	0.00065	0.0007	37.25↑	7.69↑	1459.47	1445.06	1242.36
CNN	l_2	0.00484	0.01067	0.01504	210.74↑	40.96↑	1247.22	1208.68	1237.03
4 layer	l_1	0.01393	0.03273	0.04647	233.60↑	41.98↑	1242.38	1210.06	1239.86
Tiny ImageNet	l_∞	0.00062	0.00084	0.00094	51.61↑	11.90↑	5304.63	5072.55	5489.77
CNN	l_2	0.00578	0.01036	0.01369	136.85↑	32.14↑	5176.38	5242.1	5155.05
5 layer	l_1	0.01504	0.02726	0.03616	140.43↑	32.65↑	5155.55	4945.58	5147.84
Tiny ImageNet	l_∞	0.00047	0.00058	0.00065	38.30↑	12.07↑	12459.81	11982.54	12385.09
CNN	l_2	0.00515	0.00756	0.00942	82.91↑	24.60↑	12845.13	12030	12833.63
6 layer	l_1	0.01499	0.02213	0.02808	87.32↑	26.89↑	12331.93	11896.23	12218.5

Table 9: Averaged certified robustness bounds and runtime on CNNs(ReLU) with Maxpooling tested on Tiny ImageNet by CNN-Cert, DeepPoly and Ti-Lin

Neural networks with ReLU functions Despite the focus on Sigmoid, Arctan, Tanh and Maxpooling functions, our approach is applicable to ReLU-based network, and the linear constraints is deferred in Appendix due to space limitation. The ReLU constraints

provided is also the *Neuron-wise Tightest*. However, approximation technique is not necessary for ReLU-based networks as there are other verification methods which can get accurate robustness

Dataset	Baseline Methods	p-value
MNIST	DeepCert	1.17×10^{-18}
	VeriNet	1.54×10^{-20}
	Newise	2.66×10^{-16}
CIFAR-10	DeepCert	1.37×10^{-4}
	VeriNet	1.10×10^{-2}
	Newise	9.75×10^{-14}
Dataset	Baseline Methods	p-value
MNIST	CNN-Cert	3.06×10^{-6}
	DeepPoly	3.06×10^{-6}
CIFAR-10	CNN-Cert	3.06×10^{-6}
	DeepPoly	3.06×10^{-6}
Tiny	CNN-Cert	3.48×10^{-4}
ImageNet	DeepPoly	3.48×10^{-4}

Table 10: Wilcoxon Rank-sum Test Results

bounds by using Satisfiability Modulo Theories [28] and Mixed Integer Linear Programming [31].

Neural networks with non-negative weights For such networks, Newise is the best verification techniques, which can efficiently obtain accurate certified robustness bounds. The training dataset and the number of fully-connected layers can influence the weights. When the number of fully-connected layer is only one, the variety of the weights decrease and may be prone to non-negative. However, we believe that most network are mix-weight. The reasons are listed as follows:(i) To tackle various complex tasks, the number of the fully-connected layers in networks is often more than one; (ii) Neural network are widely used in various domains, weights of the network can be quite different.

6 RELATED WORK

There is plenty of ongoing works using linear approximation to verify the robustness of convolutional neural networks against adversarial attacks, and the main challenge to verify robustness is the non-linear property of networks, that is, ReLU, Maxpool, Sigmoid/Arctan/Tanh. Moreover, abstract interpretation is also a robustness verification method, which is similar to linear approximation. We briefly introduce the similarity and difference between these two verification methods in this section. A survey on formal robustness verification with linear approximation is proposed in the work [18].

ReLU. Linear approximation of the ReLU function is firstly proposed in the work [16] by offering a pair of bounds to ReLU function instead of its piecewise feature. Fast-Lin [17] gives parallel linear bounds to ReLU function. State-of-the-art linear approximation of ReLU function is proposed in DeepPoly [4], which has the highest precision among all relevant works by producing the smallest over-approximation region of ReLU function.

Sigmoid, Arctan and Tanh. Other notable non-linear functions are Sigmoid, Arctan and Tanh functions. As these functions' shapes are similar(S-shaped), their linear constraints are the same in essence. Recent techniques for Sigmoid and Tanh functions are proposed in DeepZ [8] and DeepPoly [4]. CROWN [5] proposes a more general method that can offer non-trivial linear bounds to Sigmoid, Arctan, and Tanh functions and is extended to FROWN [9] with tighter approximation by using a gradient-based method to find the bounding lines. State-of-the-art linear approximation of Sigmoid, Arctan, and Tanh functions are proposed in VeriNet [15] and DeepCert [1], DeepCert can compute much tighter robustness bounds compared with CROWN and FROWN, while VeriNet produces a minimum over-approximation region of Sigmoid, Arctan and Tanh functions and stands for the highest precision for general CNNs. Recently, network-wise Tightest approach is proposed in Newise [22] and is the most precise method for monotonous CNNs(such as non-negative CNNs).

Maxpool. Besides ReLU, Sigmoid, Arctan, and Tanh functions, Maxpool is a non-linear function commonly used in CNNs. However, as it is a multivariate function, Maxpool is far more complex to be verified. DeepPoly [4] gives a loose linear bound to Maxpool and its parallel work, CNN-Cert [2] gives non-trivial bounds by leveraging a hyperplane containing n different particular points. 3DCertify [19] gives tighter bounds than DeepPoly by double description method and is applicable for point cloud models. However, 3DCertify's perturbation form is rotation and is not suitable for image data, which is perturbed in a l_p -norm ball.

Abstract Interpretation In the survey [26], linear approximation technique is contained in abstract interpretation domain [8, 14, 27]. The over-approximation zone is called as abstract domain in this field. In the survey [18], these two technique are divided. The similarity between abstract interpretation and linear approximation is that they both need to give a pair of upper and lower linear constraints of a non-linear function $f(x)$ in a given interval $[l, u]$. When the abstract domain of abstract interpretation is polyhedra [4], there is no essential difference between these two techniques. However, when the abstract domain is zonotope [14, 27], abstract interpretation can abandon the backsubstitution process [4] and computes faster than the linear approximation method. However, abstract interpretation has some precision loss due to its parallel linear constraints compared to linear approximation.

7 CONCLUSION

In this paper, we propose Ti-Lin, providing tight linear bounds for certifying the robustness of general CNNs. Ti-Lin applies to CNNs with Sigmoid/Tanh/Arctan/ReLU/Maxpool functions and gains tighter non-trivial certified robustness bounds with almost the same computational complexity. Concretely, Ti-Lin certifies much more precise robustness bounds on pure CNNs with Sigmoid/Tanh/Arctan functions and CNNs with Maxpooling function with at most 63.70% and 253.54% improvement, respectively. Furthermore, we illustrate the relation of tighter certified bounds and minimizing the over-approximation zone of non-linear function by introducing the notion of *Neuron-wise Tightest*. We implemented Ti-Lin in various networks on MNIST, CIFAR-10, and Tiny ImageNet datasets, including pure CNNs without any Maxpooling layer,

and CNNs with Maxpooling layers. The experimental results have shown Ti-Lin's efficiency and effectiveness.

REFERENCES

- [1] Y. Wu and M. Zhang, "Tightening robustness verification of convolutional neural networks with fine-grained linear approximation," in *Proceedings of the AAAI Conference on Artificial Intelligence*, vol. 35, no. 13, 2021, pp. 11 674–11 681.
- [2] A. Boopathy, T.-W. Weng, P.-Y. Chen, S. Liu, and L. Daniel, "Cnn-cert: An efficient framework for certifying robustness of convolutional neural networks," in *Proceedings of the AAAI Conference on Artificial Intelligence*, vol. 33, no. 01, 2019, pp. 3240–3247.
- [3] C.-Y. Ko, Z. Lyu, L. Weng, L. Daniel, N. Wong, and D. Lin, "Popqorn: Quantifying robustness of recurrent neural networks," in *International Conference on Machine Learning*. PMLR, 2019, pp. 3468–3477.
- [4] G. Singh, T. Gehr, M. Püschel, and M. Vechev, "An abstract domain for certifying neural networks," *Proceedings of the ACM on Programming Languages*, vol. 3, no. POPL, pp. 1–30, 2019.
- [5] H. Zhang, T.-W. Weng, P.-Y. Chen, C.-J. Hsieh, and L. Daniel, "Efficient neural network robustness certification with general activation functions," *Advances in neural information processing systems*, vol. 31, 2018.
- [6] M. N. Müller, G. Makarchuk, G. Singh, M. Püschel, and M. Vechev, "Prima: Precise and general neural network certification via multi-neuron convex relaxations," *arXiv preprint arXiv:2103.03638*, 2021.
- [7] T. Du, S. Ji, L. Shen, Y. Zhang, J. Li, J. Shi, C. Fang, J. Yin, R. Beyah, and T. Wang, "Cert-rnn: Towards certifying the robustness of recurrent neural networks." in *CCS*, 2021, pp. 516–534.
- [8] G. Singh, T. Gehr, M. Mirman, M. Püschel, and M. Vechev, "Fast and effective robustness certification," *Advances in neural information processing systems*, vol. 31, 2018.
- [9] Z. Lyu, C.-Y. Ko, Z. Kong, N. Wong, D. Lin, and L. Daniel, "Fastened crown: Tightened neural network robustness certificates," in *Proceedings of the AAAI Conference on Artificial Intelligence*, vol. 34, no. 04, 2020, pp. 5037–5044.
- [10] S.-M. Moosavi-Dezfooli, A. Fawzi, O. Fawzi, and P. Frossard, "Universal adversarial perturbations," in *Proceedings of the IEEE conference on computer vision and pattern recognition*, 2017, pp. 1765–1773.
- [11] C. Szegedy, W. Zaremba, I. Sutskever, J. Bruna, D. Erhan, I. Goodfellow, and R. Fergus, "Intriguing properties of neural networks," *arXiv preprint arXiv:1312.6199*, 2013.
- [12] D. Gopinath, G. Katz, C. S. Păsăreanu, and C. Barrett, "Deepsafe: A data-driven approach for assessing robustness of neural networks," in *International symposium on automated technology for verification and analysis*. Springer, 2018, pp. 3–19.
- [13] G. Goswami, N. Ratha, A. Agarwal, R. Singh, and M. Vatsa, "Unravelling robustness of deep learning based face recognition against adversarial attacks," in *Proceedings of the AAAI Conference on Artificial Intelligence*, vol. 32, no. 1, 2018.
- [14] T. Gehr, M. Mirman, D. Drachler-Cohen, P. Tsankov, S. Chaudhuri, and M. Vechev, "Ai2: Safety and robustness certification of neural networks with abstract interpretation," in *2018 IEEE symposium on security and privacy (SP)*. IEEE, 2018, pp. 3–18.
- [15] P. Henriksen and A. Lomuscio, "Efficient neural network verification via adaptive refinement and adversarial search," in *ECAI 2020*. IOS Press, 2020, pp. 2513–2520.
- [16] B. Meyer, "Soundness and completeness: With precision," *Retrieved May*, vol. 28, p. 2020, 2019.
- [17] L. Weng, H. Zhang, H. Chen, Z. Song, C.-J. Hsieh, L. Daniel, D. Boning, and I. Dhillon, "Towards fast computation of certified robustness for relu networks," in *International Conference on Machine Learning*. PMLR, 2018, pp. 5276–5285.
- [18] M. H. Meng, G. Bai, S. G. Teo, Z. Hou, Y. Xiao, Y. Lin, and J. S. Dong, "Adversarial robustness of deep neural networks: A survey from a formal verification perspective," *IEEE Transactions on Dependable and Secure Computing*, 2022.
- [19] T. Lorenz, A. Ruoss, M. Balunović, G. Singh, and M. Vechev, "Robustness certification for point cloud models," in *Proceedings of the IEEE/CVF International Conference on Computer Vision*, 2021, pp. 7608–7618.
- [20] P. Huang, Y. Yang, M. Liu, F. Jia, F. Ma, and J. Zhang, "ε-weakened robustness of deep neural networks," in *ISSTA '22: 31st ACM SIGSOFT International Symposium on Software Testing and Analysis, Virtual Event, South Korea, July 18 - 22, 2022*, S. Ryu and Y. Smaragdakis, Eds. ACM, 2022, pp. 126–138. [Online]. Available: <https://doi.org/10.1145/3533767.3534373>
- [21] Z. Zhao, G. Chen, J. Wang, Y. Yang, F. Song, and J. Sun, "Attack as defense: characterizing adversarial examples using robustness," in *ISSTA '21: 30th ACM SIGSOFT International Symposium on Software Testing and Analysis, Virtual Event, Denmark, July 11-17, 2021*, C. Cadar and X. Zhang, Eds. ACM, 2021, pp. 42–55. [Online]. Available: <https://doi.org/10.1145/3460319.3464822>
- [22] Z. Zhang, Y. Wu, S. Liu, J. Liu, and M. Zhang, "Provably tightest linear approximation for robustness verification of sigmoid-like neural networks," *arXiv preprint arXiv:2208.09872*, 2022.
- [23] Y. LeCun, "The mnist database of handwritten digits," <http://yann.lecun.com/exdb/mnist/>, 1998.
- [24] L. D. Capitani and D. D. Martini, "On stochastic orderings of the wilcoxon rank sum test statistic with applications to reproducibility probability estimation testing," *Statistics & Probability Letters*, vol. 81, pp. 937–946, 2011.
- [25] D. P. Kingma and J. Ba, "Adam: A method for stochastic optimization," *CoRR*, vol. abs/1412.6980, 2015.
- [26] S. L. Ji, T. Y. Du, S. G. Deng, P. Cheng, J. Shi, M. Yang, and B. Li, "Robustness certification research on deep learning models: A survey," *Jisuanji Xuebao/Chinese Journal of Computers*, vol. 45, no. 1, pp. 190–206, 2022.
- [27] M. Mirman, T. Gehr, and M. Vechev, "Differentiable abstract interpretation for provably robust neural networks," in *International Conference on Machine Learning*. PMLR, 2018, pp. 3578–3586.
- [28] G. Katz, C. Barrett, D. L. Dill, K. Julian, and M. J. Kochenderfer, "Reluplex: An efficient smt solver for verifying deep neural networks," in *International conference on computer aided verification*. Springer, 2017, pp. 97–117.
- [29] R. Ehlers, "Formal verification of piece-wise linear feed-forward neural networks," in *International Symposium on Automated Technology for Verification and Analysis*. Springer, 2017, pp. 269–286.
- [30] X. Huang, M. Kwiatkowska, S. Wang, and M. Wu, "Safety verification of deep neural networks," in *International conference on computer aided verification*. Springer, 2017, pp. 3–29.
- [31] V. Tjeng, K. Y. Xiao, and R. Tedrake, "Evaluating robustness of neural networks with mixed integer programming," in *International Conference on Learning Representations*, 2018.
- [32] J. Jia, B. Wang, X. Cao, and N. Z. Gong, "Certified robustness of community detection against adversarial structural perturbation via randomized smoothing," in *Proceedings of The Web Conference 2020*, 2020, pp. 2718–2724.
- [33] M. Fazlyab, M. Morari, and G. J. Pappas, "Probabilistic verification and reachability analysis of neural networks via semidefinite programming," in *2019 IEEE 58th Conference on Decision and Control (CDC)*. IEEE, 2019, pp. 2726–2731.
- [34] L. Weng, P.-Y. Chen, L. Nguyen, M. Squillante, A. Boopathy, I. Oseledets, and L. Daniel, "Proven: Verifying robustness of neural networks with a probabilistic approach," in *International Conference on Machine Learning*. PMLR, 2019, pp. 6727–6736.
- [35] S. Wang, K. Pei, J. Whitehouse, J. Yang, and S. S. Jana, "Efficient formal safety analysis of neural networks," in *NeurIPS*, 2018.

8 APPENDIX

THEOREM 8.1 (RELU LINEAR BOUNDS). Given $f(x) = \max(0, x)$, $x \in [l, u]$. Then the linear bounds are:

$$\begin{cases} u(x) = \frac{f(u) - f(l)}{u - l}(x - l) + f(l), l(x) = 0, m \leq 0 \\ u(x) = \frac{f(u) - f(l)}{u - l}(x - l) + f(l), l(x) = x, m > 0 \end{cases}$$

Define $[n_k^+] = \{i | w_i^k > 0\}$ and $[n_k^-] = \{i | w_i^k < 0\}$

PROOF:NEURON-WISE TIGHTEST IS EQUIVALENT TO LAYER-WISE TIGHTEST. We define linear bounds are *Layer-wise Tighest* is when

$$\iint_{x \in \times_{q \in [n_{k-1}]} [l_q^{k-1}, u_q^{k-1}]} (\sum_{i \in [n_k^+]} W_{ji}^{+,k+1} u_i^k(x) - \sum_{i \in [n_k^-]} W_{ji}^{-,k+1} l_i^k(x)) dx \text{ is minimal.}$$

As $l_q^{k-1}, u_q^{k-1}, W_{ji}^{+,k+1}, W_{ji}^{-,k+1}$ are constant and $[n_k^+] \cap [n_k^-] = \emptyset$, thus we need to minimize $\iint_{x \in \times_{q \in [n_{k-1}]} [l_q^{k-1}, u_q^{k-1}]} u_i^k(x) dx, i \in [n_k^+]$ and $\iint_{x \in \times_{q \in [n_{k-1}]} [l_q^{k-1}, u_q^{k-1}]} (-l_i^k(x)) dx, i \in [n_k^-]$ respectively. \square

PROOF:NEURON-WISE TIGHTEST LINEAR BOUNDS. Because $u_i^k(x)$ is a linear combination of x . Without loss of generality, we assume $u_i^k(x) = u_i^k(x_1, \dots, x_{n_{k-1}}) = \sum_{q \in [n_{k-1}]} a_{u,iq}^k x_q + b_{u,i}^k$. Then,

$$\begin{aligned} & \iint_{x \in \times_{q \in [n_{k-1}]} [l_q^{k-1}, u_q^{k-1}]} u_i^k(x) dx \\ &= \iint_{x \in \times_{q \in [n_{k-1}]} [l_q^{k-1}, u_q^{k-1}]} \left(\sum_{q \in [n_{k-1}]} a_{u,iq}^k x_q + b_{u,i}^k \right) dx \\ &= \sum_{q \in [n_{k-1}]} \frac{a_{u,iq}^k}{2} ((u_q^{k-1})^2 - (l_q^{k-1})^2) + b_{u,i}^k (u_q^{k-1} - l_q^{k-1}) \\ &= (u_q^{k-1} - l_q^{k-1}) \left(\sum_{q \in [n_{k-1}]} a_{u,iq}^k \frac{u_q^{k-1} + l_q^{k-1}}{2} + b_{u,i}^k \right) \\ &= (u_q^{k-1} - l_q^{k-1}) u_i^k(m) \end{aligned}$$

where $m = \left(\frac{u_1^{k-1} + l_1^{k-1}}{2}, \dots, \frac{u_{n_{k-1}}^{k-1} + l_{n_{k-1}}^{k-1}}{2} \right)$, because $u_q^{k-1}, l_q^{k-1}, q \in [n_{k-1}]$ are constant, and the minimize target has been transformed into minimizing $u_i^k(m), i \in [n_k^+]$.

Symmetric to the proof of minimizing $\iint_{x \in \times_{q \in [n_{k-1}]} [l_q^{k-1}, u_q^{k-1}]} u_i^k(x) dx$, minimizing $-\iint_{x \in \times_{q \in [n_{k-1}]} [l_q^{k-1}, u_q^{k-1}]} l_i^k(x) dx, i \in [n_k^-]$ is equivalent to minimizing $-l_i^k(m), i \in [n_k^-]$.

And symmetric to the above proof, minimizing $-\iint_{x \in \times_{q \in [n_{k-1}]} [l_q^{k-1}, u_q^{k-1}]} (\sum_{i \in [n_k^+]} W_{ji}^{+,k+1} l_i^k(x) - \sum_{i \in [n_k^-]} W_{ji}^{-,k+1} u_i^k(x)) dx$, is equivalent to $-l_i^k(m), i \in [n_k^+], u_i^k(m), i \in [n_k^-]$.

This completes the proof. \square

Here, we provide a way to find Neuron-wise Tighest linear bounds of non-linear function $f(x)$.

In essence, the theorem "Finding Neuron-wise Tighest Linear Bounds" shows that if the tangent line/plane at m is the upper/lower bound of $f(x)$, then the tangent line/plane at $x = m$ is obviously the Neuron-wise Tighest linear upper/lower bound of $f(x)$. Otherwise, we try to find two points that satisfy $m = \lambda d_1 + (1 - \lambda) d_2, \lambda \in [0, 1]$, so that if a line/plane passing through $(d_1, f(d_1)), (d_2, f(d_2))$ is the linear bound of $f(x)$, then this line/plane is the Neuron-wise Tighest bounding constraints.

PROOF:FINDING NEURON-WISE TIGHTEST LINEAR BOUNDS. Obviously, (1) is right.

And we prove (2) by contradiction. Without loss of generality, we suppose the line/plane to be proved is an upper bound $u(x)$ and $u(d_1) = f(d_1), u(d_2) = f(d_2), m = \lambda d_1 + (1 - \lambda) d_2, \lambda \in [0, 1]$. We assume there is another bounding line/plane $u'(x)$ and $u'(m) < u(m)$. Because $u(x), u'(x)$ are linear combinations of x and $m = \lambda d_1 + (1 - \lambda) d_2, \lambda \in [0, 1]$, then $u(m) = \lambda u(d_1) + (1 - \lambda) u(d_2), u'(m) = \lambda u'(d_1) + (1 - \lambda) u'(d_2), \lambda \in [0, 1]$. Therefore, $\lambda u'(d_1) + (1 - \lambda) u'(d_2) < \lambda u(d_1) + (1 - \lambda) u(d_2) = \lambda f(d_1) + (1 - \lambda) f(d_2)$ which contradicts $u'(d_1) \geq f(d_1), u'(d_2) \geq f(d_2)$.

This completes the proof. \square

PROOF:SIGMOID/TANH/ARCTAN LINEAR BOUNDS. $m = F^k(x_0) \in [l, u] \in \mathbb{R}$, and if $d_1 \leq m \leq d_2$, then there exists $\lambda = \frac{d_2 - m}{d_2 - d_1}$, s.t. $\lambda d_1 + (1 - \lambda) d_2 = m$

case 1: $m \geq 0$

upper bound:

(1) when $k_{ml} > f'(m)$:

As $m \geq 0$, we have $u \geq 0$, and when $x \geq 0$, $f(x)$ is concave. Therefore, $f(x) \leq f'(m)(x - m) + f(m)$, $x \in [m, u]$.

Considering $x < 0$, because $k_{ml} > f'(m)$, we have $f'(m)(l - m) + f(m) > k_{ml}(l - m) + f(m) = f(l)$ and $f'(m)(l - m) + f(m) \geq f(0)$.

Thus, as $f(x)$, $x < 0$ is convex, then $f'(m)(l - m) + f(m) \geq f(x)$

Thus, $f'(m)(x - m) + f(m)$ is the upper bounding line and $u(m)$ is minimum obviously, by theorem 3.4(1).

(2) when $k_{ml} < f'(m)$ and $k > f'(u)$:

$k > f'(u)$, means the tangent point x^* exists. Because $f(x)$ is continuous, $f'(0) > \frac{f(0)-f(l)}{0-l}$ and $f'(u) < \frac{f(u)-f(l)}{u-l}$, thus there exists a solution $x^* \in [0, u]$ for equation $f'(x^*) = \frac{f(x^*)-f(l)}{x^*-l}$.

$k_{ml} < f'(m)$, means $m \in [l, x^*]$. Because $k_{ml} < f'(m)$ and $f'(u) < \frac{f(u)-f(l)}{u-l}$, thus $m < x^* < u$. Because $f(x)$, $x \geq 0$ is concave, $f(x) \leq f'(x^*)(x - x^*) + f(x^*)$, $x \geq 0$. Because $f'(x^*)(0 - x^*) + f(x^*) \geq f(0)$, $f'(x^*)(l - x^*) + f(x^*) = f(l)$ and $f(x)$, $x < 0$ is convex, thus $f'(x^*)(x - x^*) + f(x^*) \geq f(x)$, $x < 0$

Therefore, $f'(x^*)(x - x^*) + f(x^*)$ is the upper bound, and as $l \leq m < x^*$, by theorem 3.4(2), $u(m)$ reaches minimum.

(3) when $k_{ml} < f'(m)$ and $k \leq f'(u)$:

$k \leq f'(u)$, which means $k(x - l) + f(l) \geq f(x)$. Because when $x > 0$, we have $k(x - l) + f(l) = k(x - u) + f(u) > f'(u)(x - u) + f(u)$ and $f(x)$, $x > 0$ is concave, thus $k(x - l) + f(l) \geq f(x)$, $x > 0$. When $x \leq 0$, we have $k \leq f'(u) < \frac{f(0)-f(u)}{0-u}$, thus $k(0 - u) + f(u) > \frac{f(0)-f(u)}{0-u}(0 - u) + f(u) = f(0)$. As $f(x)$ is convex when $x \leq 0$. Thus $k(x - l) + f(l)$ is the upper bound and as $m \in [l, u]$, $u(m)$ reaches minimum by Theorem 3.4(2).

lower bound:

(4) when $k \geq f'(l)$,

As proved above, $k \geq f'(l)$ means the tangent point x^{**} exists and the $f'(x^{**})(x - u) + f(u)$ is the lower bound. As $u \geq m > 0 > x^{**}$, $l(m)$ reaches its minimum by Theorem 3.4(2).

(5) when $k < f'(l)$,

As proved above, $k(x - l) + f(l)$ is the lower bound and as $l \leq m \leq u$, $l(m)$ achieves it minimum by theorem 3.4(2).

case 2: $m < 0$ The proof of case 2 is symmetric to the proof of case 1, for the reason that $f(x)$ is centrosymmetry about the origin. \square

Similar to proof " Sigmoid/Tanh/Arctan Linear Bounds" , when $m = \frac{u+l}{2}$, the linear bounds of theorem 3.1 is Neuron-wise Tightest according to theorem 3.4 and theorem 3.2. Although the Neuron-wise Tightest technique [15] can compute a larger robustness bounds than other state-of-the-art works and stands for the highest precision among related work, experimental results have shown that Ti-Lin is better than the Neuron-wise Tightest linear bounds of Sigmoid/Tanh/Arctan function.

PROOF:MAXPOOL LINEAR BOUNDS. $m = (m_1, \dots, m_n) \in \mathbb{R}^n$.

upper bound:

case 1: When $u_i \geq l_j \geq \dots$, $f(x_1, \dots, x_n) = x_i, \forall (x_1, \dots, x_n)$, then we set $u(x_1, \dots, x_n) = x_i$, then $u(m) = f(m)$ which is the Neuron-wise Tightest upper bounding plane by Theorem 3.4(1).

case 2: When $u_i \geq u_j \geq l_j \geq \dots$, $f(x_1, \dots, x_n) = \max(x_i, x_j), \forall (x_1, \dots, x_n)$.

If $f(x_1, \dots, x_n) = x_i$,

$$\begin{aligned}
 u(x_1, \dots, x_n) - x_i &= \frac{u_i - l_j}{u_i - l_i}(x_i - l_i) + (x_j - l_j) + l_j - x_i \\
 &= \frac{u_i - l_j}{u_i - l_i}(x_i - l_i) + (x_j - l_j) + l_j - l_i + l_i - x_i \\
 &= (x_i - l_i)\left(\frac{u_i - l_j}{u_i - l_i} - 1\right) + (x_j - l_j) + l_j - l_i \\
 &= (x_i - l_i)\frac{l_i - l_j}{u_i - l_i} + (x_j - l_j) + l_j - l_i \\
 &= (l_j - l_i)\left(1 - \frac{x_i - l_i}{u_i - l_i}\right) + (x_j - l_j) \\
 &= (l_j - l_i)\frac{u_i - x_i}{u_i - l_i} + (x_j - l_j) \\
 &\geq 0
 \end{aligned}$$

If $f(x_1, \dots, x_n) = x_j$,

$$\begin{aligned} u(x_1, \dots, x_n) - x_j &= \frac{u_i - l_j}{u_i - l_i}(x_i - l_i) + (x_j - l_j) + l_j - x_j \\ &= \frac{u_i - l_j}{u_i - l_i}(x_i - l_i) \\ &\geq 0 \end{aligned}$$

Because

$$\begin{aligned} u(u_1, \dots, u_{i-1}, u_i, u_{i+1}, \dots, u_{j-1}, l_j, u_{j+1}, \dots, u_n) &= \frac{u_i - l_j}{u_i - l_i}(u_i - l_i) + (l_j - l_j) + l_j \\ &= u_i - l_j + l_j \\ &= f(u_1, \dots, u_{i-1}, u_i, u_{i+1}, \dots, u_{j-1}, l_j, u_{j+1}, \dots, u_n) \end{aligned}$$

and

$$\begin{aligned} u(l_1, \dots, l_{i-1}, l_i, l_{i+1}, \dots, l_{j-1}, u_j, l_{j+1}, \dots, l_n) &= \frac{u_i - l_j}{u_i - l_i}(l_i - l_i) + (u_j - l_j) + l_j \\ &= u_j - l_j + l_j \\ &= f(l_1, \dots, l_{i-1}, l_i, l_{i+1}, \dots, l_{j-1}, u_j, l_{j+1}, \dots, l_n) \end{aligned}$$

we notice that $(u_1, \dots, u_{i-1}, u_i, u_{i+1}, \dots, u_{j-1}, l_j, u_{j+1}, \dots, u_n)$ and $(l_1, \dots, l_{i-1}, l_i, l_{i+1}, \dots, l_{j-1}, u_j, l_{j+1}, \dots, l_n)$ are the space diagonal of $\times_{i=1}^n [l_i, u_i]$, and $m = \frac{1}{2}(u_1, \dots, u_{i-1}, u_i, u_{i+1}, \dots, u_{j-1}, l_j, u_{j+1}, \dots, u_n) + \frac{1}{2}(l_1, \dots, l_{i-1}, l_i, l_{i+1}, \dots, l_{j-1}, u_j, l_{j+1}, \dots, l_n)$, thus the plane is the Neuron-wise Tightest linear upper plane by Theorem 3.4(2).

case 3: When $u_i \geq u_j \geq u_k \geq \dots$, $f(x_1, \dots, x_n) = \max(x_1, \dots, x_n)$, $\forall (x_1, \dots, x_n)$. If $f(x_1, \dots, x_n) = x_i$,

$$\begin{aligned} u(x_1, \dots, x_n) - x_i &= \frac{u_i - u_k}{u_i - l_i}(x_i - l_i) + \frac{u_j - u_k}{u_j - l_j}(x_j - l_j) + u_k - x_i \\ &= \frac{u_i - u_k}{u_i - u_k}(x_i - l_i) + \frac{u_j - u_k}{u_j - l_j}(x_j - l_j) + u_k - l_i + l_i - x_i \\ &= (x_i - l_i)\left(\frac{u_i - u_k}{u_i - l_i} - 1\right) + \frac{u_j - u_k}{u_j - l_j}(x_j - l_j) + u_k - l_i \\ &= (x_i - l_i)\frac{l_i - u_k}{u_i - l_i} + \frac{u_j - u_k}{u_j - l_j}(x_j - l_j) + u_k - l_i \\ &= (u_k - l_i)\left(1 - \frac{x_i - l_i}{u_i - l_i}\right) + \frac{u_j - u_k}{u_j - l_j}(x_j - l_j) \\ &= (u_k - l_i)\frac{u_i - x_i}{u_i - l_i} + \frac{u_j - u_k}{u_j - l_j}(x_j - l_j) \\ &\geq 0 \end{aligned}$$

If $f(x_1, \dots, x_n) = x_j$, the proof is the same as above.

$$\begin{aligned} u(x_1, \dots, x_n) - x_j &= \frac{u_i - u_k}{u_i - l_i}(x_i - l_i) + \frac{u_j - u_k}{u_j - l_j}(x_j - l_j) + u_k - x_j \\ &= \frac{u_i - u_k}{u_i - u_k}(x_i - l_i) + \frac{u_j - u_k}{u_j - l_j}(x_j - l_j) + u_k - l_j + l_j - x_j \\ &= \frac{u_i - u_k}{u_i - l_i}(x_i - l_i) + \left(\frac{u_j - u_k}{u_j - l_j} - 1\right)(x_j - l_j) + u_k - l_j \\ &= \frac{u_i - u_k}{u_i - l_i}(x_i - l_i) + \frac{l_j - u_k}{u_j - l_j}(x_j - l_j) + u_k - l_i \\ &= \frac{u_i - u_k}{u_i - l_i}(x_i - l_i) + \left(1 - \frac{x_j - l_j}{u_j - l_j}\right)(u_k - l_j) \\ &= \frac{u_i - u_k}{u_i - l_i}(x_i - l_i) + \frac{u_j - x_j}{u_j - l_j}(u_k - l_j) \\ &\geq 0 \end{aligned}$$

If $f(x_1, \dots, x_n) = x_k$,

$$\begin{aligned} u(x_1, \dots, x_n) - x_j &= \frac{u_i - u_k}{u_i - l_i}(x_i - l_i) + \frac{u_j - u_k}{u_j - l_j}(x_j - l_j) + (u_k - x_k) \\ &\geq 0 \end{aligned}$$

If $f(x_1, \dots, x_n) = x_l, l \neq i, j, k,$

$$\begin{aligned} u(x_1, \dots, x_n) - x_l &= \frac{u_i - u_k}{u_i - l_i}(x_i - l_i) + \frac{u_j - u_k}{u_j - l_j}(x_j - l_j) + u_k - x_l \\ &= \frac{u_i - u_k}{u_i - l_i}(x_i - l_i) + \frac{u_j - u_k}{u_j - l_j}(x_j - l_j) + (u_k - u_l) + (u_l - x_l) \\ &\geq 0 \end{aligned}$$

Because

$$\begin{aligned} u(u_1, \dots, u_{i-1}, u_i, u_{i+1}, \dots, u_{j-1}, l_j, u_{j+1}, \dots, u_n) &= \frac{u_i - u_k}{u_i - l_i}(u_i - l_i) + \frac{u_j - u_k}{u_j - l_j}(l_j - l_j) + u_k \\ &= u_i - u_k + u_k \\ &= f(u_1, \dots, u_{i-1}, u_i, u_{i+1}, \dots, u_{j-1}, l_j, u_{j+1}, \dots, u_n) \end{aligned}$$

and

$$\begin{aligned} u(l_1, \dots, l_{i-1}, l_i, l_{i+1}, \dots, l_{j-1}, u_j, l_{j+1}, \dots, l_n) &= \frac{u_i - u_k}{u_i - l_i}(l_i - l_i) + \frac{u_j - u_k}{u_j - l_j}(u_j - l_j) + u_k \\ &= u_j - u_k + u_k \\ &= f(l_1, \dots, l_{i-1}, l_i, l_{i+1}, \dots, l_{j-1}, u_j, l_{j+1}, \dots, l_n) \end{aligned}$$

$m = \frac{1}{2}(u_1, \dots, u_{i-1}, u_i, u_{i+1}, \dots, u_{j-1}, l_j, u_{j+1}, \dots, u_n) + \frac{1}{2}(l_1, \dots, l_{i-1}, l_i, l_{i+1}, \dots, l_{j-1}, u_j, l_{j+1}, \dots, l_n),$ by Theorem 3.4(2), the upper bound is the Neuron-wise Tightest bounding plane.

lower bound:

$$l(x_1, \dots, x_n) = x_j = \operatorname{argmax}_i m_i, \text{ and } \forall (x_1, \dots, x_n) \in \times_{i=1}^n [l_i, u_i],$$

$$\begin{aligned} f(x_1, \dots, x_n) &= \max(x_1, \dots, x_n) \\ &\geq x_j \\ &= l(x_1, \dots, x_n) \end{aligned}$$

Furthermore, $l(m) = f(m_1, \dots, m_n),$ hence, $l(x_1, \dots, x_n)$ is the Neuron-wise Tightest lower bounding plane by Theorem 3.4(1).

This completes the proof. \square